Liquid crystal elastomers based upon cellulose derivatives

G. R. Mitchell, W. Guo and F. J. Davis
Polymer Science Centre, University of Reading, Whiteknights, Reading RG6 2AF, UK
(Received 5 November 1990; accepted 28 January 1991)

Crosslinked networks displaying both thermotropic and lyotropic liquid crystalline phases have been prepared from hydroxypropyl cellulose. The phase transitions from the liquid crystal to isotropic state are reversible for materials with moderate levels of crosslinking. These materials show characteristic optical textures similar to uncrosslinked cellulose-based liquid crystal polymers although well defined patterns typical of cholesteric structures were not observed. The samples were insoluble in water, but high levels of swelling with acetone and benzene were observed and in the steady state condition a lyotropic phase was present even though the level of swelling was in excess of 500%. A reversible liquid crystalline to isotropic phase was observed with the swollen materials as the fraction of swellant was adjusted. The elastomers show marked global orientation effects when mechanically deformed but surprisingly the response was less dramatic than in some side-chain liquid crystal elastomers.

(Keywords: liquid crystal elastomers; cellulose; orientation)

INTRODUCTION

The introduction of a three-dimensional crosslinked network into a liquid crystalline organization results in materials with most interesting and unusual properties. The interaction between the network and the mesomorphic structure can result in electric field induced shape changes[1,2] stress induced molecular switching[2–5] and marked variation in phase behaviour[6,7]. A variety of main chain and side chain based thermotropic liquid crystal elastomers have been prepared[8–10]. Here we report the extension of these concepts to a cellulose-based lyotropic–thermotropic liquid crystal system. Studies of side-chain liquid crystal elastomers swollen with low molar mass mesomorphic compounds have been detailed[1,2,11], and liquid crystal phases observed with high level of swelling (> 50% by volume) at temperatures above the clearing point for the swellant. However, it is more appropriate to consider these materials to be mixtures of mesogenic materials. In this study we are concerned with cellulose derivatives which form lyotropic liquid crystal phases, often cholesteric, in a wide range of solvents for differing substituents[12–14]. In general the 'stiff' cellulose backbone gives highly anisotropic molecules which form lyotropic phases at minimum concentrations of 30–40% w/v, the particular value being dependent upon the precise solvent/derivative combination[13]. The addition of both aromatic and aliphatic side groups to the basic cellulose chain gives polymers which exhibit thermotropic liquid crystal behaviour, in which these side groups behave in effect as a solvent[15,16]. This contribution focuses on such materials into which a permanent chemically crosslinked network has been introduced and which still exhibit both lyotropic and thermotropic mesomorphic behaviour.

0032-3861/92/010068-07

MATERIALS

Bhadani and Gray[17] have prepared heavily crosslinked 'cholesteric' networks by reacting hydroxypropyl cellulose with acryloyl chloride and stimulating crosslinking between the adjacent side groups using ultraviolet radiation. The resultant films retained their static cholesteric structure, but decomposed before reaching any cholesteric–isotropic phase transition. Similar types of films in which the cholesteric structure has been permanently locked in have been prepared by a number of differing techniques, as in reference 18. We have followed a different route which allows the level of crosslinking to be controlled through competitive esterification. In essence the problem of preparing a sample with a regulated low level of crosslinking of 1–2% arises from the high concentration of reactive hydroxy sites on the hydroxypropyl cellulose chains. Reports in the literature[19] on the number of hydroxypropyl groups per anhydroglucose unit vary from three to four, and some of these obviously form multiple side chains. The addition of any multifunctional crosslinking group to such a system will inevitably lead to considerable levels of intrachain linkages and although such linkages will clearly modify the properties of the cellulose derivative they will not result in controlled interchain crosslinking. Our approach has been to partially substitute these reactive sites using a monofunctional group. Crosslinking is achieved by further reaction with a difunctional unit such as adipoyl chloride. These reactions may be either performed in a sequential manner or through reaction with a rationed mixture. For both routes it may be advantageous to maximize esterification of the polymer repeat units using an excess of the monofunctional group in a final reaction step. The samples of crosslinked

propanoated hydroxypropyl cellulose discussed here were prepared as follows: to 5 g of hydroxypropyl cellulose (Hercules Grade H) dissolved in 250 cm^3 tetrahydrofuran containing ~10 cm^3 triethylamine at 0°C was added dropwise 2 molar equivalents (meq) of propanol chloride; the mixture was then stirred for 1 h at room temperature. Crosslinking was then introduced into the system by the addition to this partially propanoated hydroxypropyl cellulose of varying quantities of adipoyl chloride, as described above; finally an attempt was made to react the remaining hydroxy groups by addition of excess (~5meq) propanoyl chloride and stirred overnight. The solvent and unreacted reagents were then removed and the resulting rubbery solid was washed first with water, then with acetone and finally repeatedly with water. The material was then dried in a vacuum overnight. Infra-red (i.r.) spectroscopy showed peaks indicating ester substitution although there remained some hydroxyl groups resulting from incomplete esterification. As an alternative route, in an attempt to attain complete substitution, esterification in pyridine was undertaken in a similar manner. However this second route offers little advantage and removal of the excess pyridine from the resultant elastomers was found to be difficult. Using these procedures a series of samples (*Figure 1*) were prepared in which the nominal ratio of adipoyl chloride to propanoyl chloride in the feedstock was varied from 0 to 0.20 as shown in *Table 1*. From i.r. spectra an estimate of the total level of esterification, i.e. both the mono- and difunctional units, was made. There was a small decrease in esterification as the proportion of difunctional unit in the feedstock was increased (*Table 1*). These measurements do not indicate the relative proportions of the mono- and difunctional units incorporated into the final films. The physical nature of the resulting elastomer was dependent upon both the level of crosslinking and the degree of substitution with additional propanoyl chains. For high levels of crosslinking the material was rigid and immobile. Such samples will not be discussed here. Networks prepared with a relatively low fraction of crosslinking units gave samples which were flexible and in some cases tacky at room temperature.

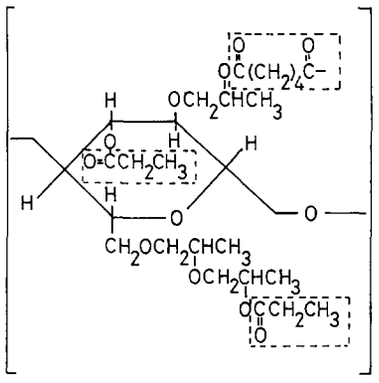

Figure 1 Schematic representation of a typical repeat unit in the synthesized material illustrating the complexity of the chemical configuration of the liquid crystal elastomers prepared in this study. The units enclosed in boxes are those added, in the reactions described in the text, to the existing hydroxypropyl cellulose chain shown with a molar degree of etherification of 3. One propanoate chain has been added directly to an unsubstituted hydroxyl unit on the ring, while another has reacted onto a double hydroxypropyl chain. The crosslinking unit (top box) has bonded to a single hydroxypropyl chain. This figure only gives a representation, many other configurations of the substitutions are possible and occur at random

Table 1 Chemical characteristics of the polymers prepared

Polymer reference	Ratio of adipoyl chloride/ propanoyl chloride in feedstock	Fraction of total esterification[a]
A	0.00	0.60
B	0.02	0.59
C	0.05	0.58
D	0.10	0.49
E	0.20	0.51

[a]Measured by Fourier transform infra-red spectroscopy

EXPERIMENTAL

Optical microscopy

Polarized light microscopy was employed to evaluate both the phase type and the phase transitions. A Carl Zeiss polarized light microscope equipped with a Linkam 900 thermal stage was used. A photodiode which replaced one of the eyepieces and connected via an amplifier to a microcomputer system was used to measure the intensity of transmitted light as a function of the thermal stage temperature. From such thermo-optic curves (heating rate 10°C min^{-1}) the liquid crystal to isotropic phase transitions were determined. Thin slices of the polymer systems, both swollen and unswollen were examined sandwiched between glass cover slides.

Thermal analysis

The materials prepared were examined using differential scanning calorimetry (Perkin-Elmer DSC-II) at a heating rate of 20°C min^{-1} using a sample weight of ~10 mg. Each sample was run at least three times.

Ultraviolet–visible spectroscopy

The most striking characteristic of the cholesteric liquid crystal phase is that of the wavelength selective reflection of light. The presence and pitch of the cholesteric helical structure may be assessed through the optical absorption characteristics of thin films of the materials. Such absorption spectra in the range (300–700 nm) were recorded using an ultraviolet (u.v.)–visible spectrophotometer (Perkin Elmer 330). Samples were examined as a function of temperature in the unswollen state using a regulated thermal stage.

Infra-red spectroscopy

A Nicolet Fourier transform infra-red spectrometer 5PC was used at a resolution of 2 cm^{-1} to estimate the esterification ratio. Hydroxyethylacrylate was used as a standard for comparison of the hydroxy to carbonyl ratio.

Swelling

Two sets of swelling experiments were performed both using benzene as the swellant at room temperature. The first set was concerned with evaluating the maximum swelling ratio and was performed using samples of known mass in a large excess of the swellant. An additional series of experiments were conducted in order to examine the

liquid crystal behaviour as a function of swellant concentration. This was achieved by preparing a series of samples with known mass/volume ratios of elastomer and solvent.

Mechanical properties

The mechanical properties of the unswollen elastomers were obtained using a miniature tensile testing machine (Rosand Precision Ltd) fitted with a 20 N force transducer and coupled to a microcomputer system for control and for recording of force–strain data. The samples were held within a temperature controlled hot-air oven (20–200°C) and the whole assembly mounted on optical track which allowed *in situ* microscopic examination during deformation. Thin films for mechanical testing were prepared by pressing at 140°C followed by annealing at 150°C to allow the material to completely relax. Samples ($\sim 5 \times 12 \times 0.3\ mm^3$) were cut from such prepared films. A strain rate of $10^{-2}\ s^{-1}$ was utilized for all experiments. An estimate was made of the effective crosslink density by utilizing the initial modulus (G) of the elastomers in the isotropic phase through the expression:

$$M_s = \frac{\rho RT}{G} \quad (1)$$

where M_s is the molecular weight between crosslink points, ρ the bulk density, R the gas constant and T is temperature. The molecular organization of the deformed samples was monitored by using wide-angle X-ray scattering procedures.

X-ray scattering measurements

The X-ray scattering measurements utilized a computer-controlled three-circle diffractometer operating in the symmetrical transmission mode and equipped with an incident beam monochromator and a Cu Kα X-ray source[4]. The scattered X-ray intensity was measured over a scattering vector range $s = 0.2–6.2\ Å^{-1}$ ($s = 4\pi \sin\theta/\lambda$, 2θ is the angle between the incident and scattered beams and λ is the incident wavelength) in steps of $0.05\ Å^{-1}$. For samples with a preferred global orientation, the scattered intensity was also measured as a function of α, the angle between the symmetry axis of the sample (the extension axis) and the normal to the plane containing incident and scattered beams. Those measurements were made from $\alpha = 0$ to 90° in steps of $\Delta\alpha = 9°$ at a fixed value of the scattering vector s. The procedures used to derive the orientation parameter $\langle P_2 \rangle$, where $\langle P_2 \rangle = (3\cos^2\alpha - 1)/2$ and α is the angle between the molecular axis and the extension direction, from these X-ray scattering intensities values are detailed elsewhere[20,21]. The majority of the experimental X-ray data reported here were obtained at room temperature on samples that had been rapidly cooled by an air jet from the experimental deformation temperature. The onset of the glass transition ensured that the static molecular organization characteristic of the liquid crystal phase at the experimental temperature was retained upon cooling. The efficacy of this approach was evaluated by performing some *in situ* scattering measurements, in which the microtensometer and oven were mounted in the diffractometer[22], an arrangement which still allowed the angle α between the extension axis and the scattering vector to be varied from 0 to 90°. Orientation parameters obtained in this manner matched those derived from room temperature scattering data.

RESULTS

Examination of the series of samples prepared as described above using a polarizing optical microscope revealed birefringent textures at room temperature for all samples, i.e. with nominal adipate/propanoate ratios of 0, 0.02, 0.05, 0.10 and 0.20. For the latter two samples, this birefringent texture remained upon heating until decomposition and no phase transition to an isotropic state was observed. For the samples with lower adipate fractions (A, B, C) the birefringent texture varied with temperature and eventually disappeared over a rather broad range of temperatures as listed in *Table 2*. This disappearance of the birefringence texture on heating indicates a transition to an isotropic phase. For the samples with adipate/propanoate ratio of 0.05 the transition was broader and less obvious than for the uncrosslinked sample A and the lightly crosslinked sample B. For the samples with adipate/propanoate fractions of 0, 0.02 and 0.05 which displayed the liquid crystal to isotropic phase transition, the reverse transition from isotropic to anisotropic states was observed. This phase transition behaviour showed considerable hysteresis. There was no evidence in the optical textures of a cholesteric phase through for example the development of 'finger print' textures even though samples were held at elevated temperatures for substantial periods of time. Differential scanning calorimetry was also used to obtain phase transition data. Transitions in broad agreement with the thermo-optic analysis were observed centred around 175°C. It was noticeable that with increasing adipate concentration that the endotherm became broad and difficult to discern. The broadening of these phase transitions appears to reflect a perhaps not surprising increase in the structural inhomogeneity with increasing crosslinking density. The lightly crosslinked samples with adipate/propanoate ratios of 0.02, 0.05 and 0.1 showed a very slight iridescence indicating the possibility of the presence of a cholesteric structure. Thin films placed between glass slides showed a broad and weak optical absorption maximum centred at ~478 nm. The absorption maximum is neither shifted when the sample is stretched by 200–300%, nor changed by increasing temperatures within the liquid crystal range. However, on heating into the isotropic phase the absorption peak was lost but it was regained on cooling. These observations suggest the presence of a cholesteric phase albeit weak or only stable in a small fraction of the material. The observed optical

Table 2 Phase transition data for a series of liquid crystal elastomers

Polymer	Crosslinking density[a] (%)	Liquid crystal–isotropic transition (°C)
A	0	135–165
B	1.6	155–190
C	1.7	180–205[b]
D	3.0	–[c]
E	5.8	–[c]

[a]Calculated from initial modulus measurements
[b]Some decomposition of sample
[c]No phase transition observed

Table 3 Crosslink density data

Polymer reference	Modulus (kN m^{-2})	M_s[a]	Crosslink density calculated from modulus[b] (%)	Crosslink density calculated from fraction of esterification (%)
A				
B	8.2	5100	1.6	1.2
C	8.9	4600	1.7	2.9
D	15.5	2700	3.0	4.9
E	30.7	1400	5.8	10.2

[a]Calculated from the modulus measurements using equation (1)
[b]Here the crosslink density is the ratio of crosslinked points to crosslinkable points

absorption maximum is in a slightly different position to that observed by Tseng *et al.*[15], a fact which probably reflects the differing levels of esterification.

The physical nature of the materials prepared suggested that a significant proportion of the adipate units had been incorporated as effective interchain crosslinks. This is confirmed by the results of the mechanical property measurements on the elastomers in the isotropic phase. From mechanical stretching experiments the Young's modulus of each material in the isotropic phase was measured and the results are shown in *Figure 2*. As expected an almost linear increase of the modulus of the material with increasing adipoyl fraction in the feedstock is observed. The calculated crosslinking densities from the measured modulus data are listed in *Table 3*. Of course such an analysis may be inappropriate for these complex materials with the possible influence of entanglements and hydrogen bonding. However it is reasonable to assume that such factors would be reasonably constant in the series considered here. It would appear that apart from the lowest level of crosslinking the efficiency of crosslinking remains approximately constant and hence the level of effective crosslinking reflects the fraction of difunctional units in the feedstock. It may be seen from *Table 3* that the introduction of higher levels of crosslinking (samples D and E) leads to a reduction in the total level of esterification. This presumably reflects the difficulty of completing the third stage of the reactions, the final esterification with a monofunctional unit as described in the Materials section, once a significant number of crosslinks are in place. The reduction in the esterification ratio for samples D and E is clearly not due to a reduction in the level of crosslinking as may be seen from the linear relationship shown in *Figure 2* between modulus and fraction of crosslinking units in the feedstock. These observations clearly demonstrate the advantages of control in the three-stage processing described above. The crosslinked polymer was insoluble in acetone, water and xylene; however, in acetone and benzene the material swelled considerably.

Figure 3 shows the X-ray scattering data obtained for the series of samples at room temperature. The diffuse scattering is compatible with the presence of a liquid crystal structure. There is no evidence of sharp 'Bragg-like' peaks which would indicate a microcrystalline structure to account for the birefringent textures. The maxima at $s = 0.5$ Å^{-1} arise from the spatial correlations between neighbouring molecules and depends upon the nature and level of the substituents. It

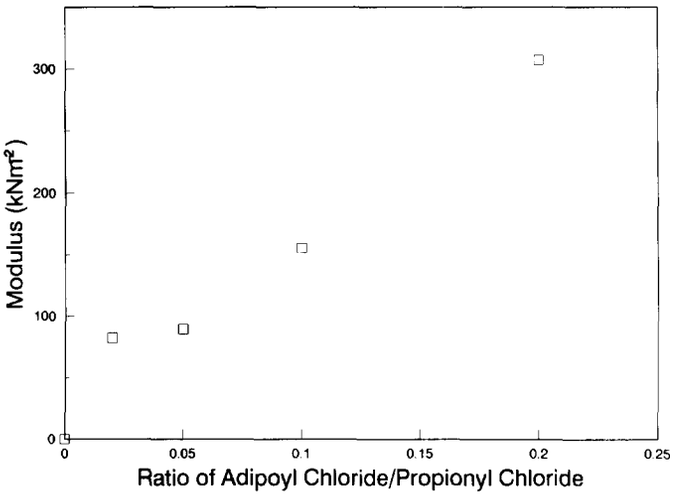

Figure 2 A plot of Young's modulus against the crosslinking density at a temperature of 180°C in the isotropic phase for the series of elastomers prepared

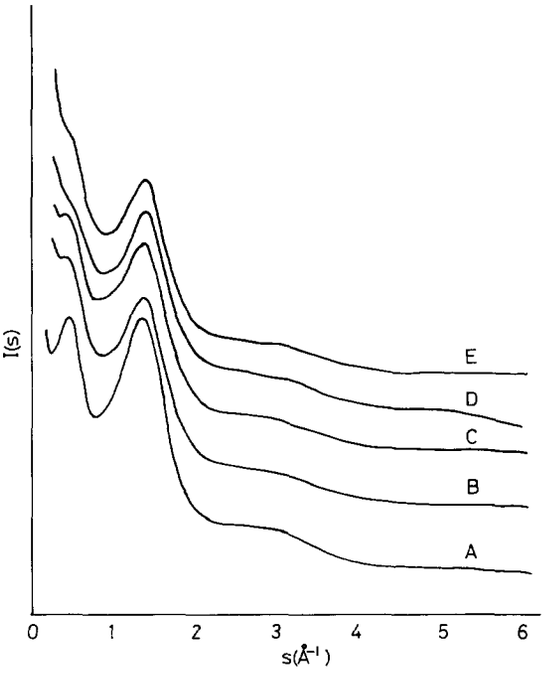

Figure 3 X-ray scattering curves for samples of different crosslinking density measured at room temperature. See *Table 1* for key

occurs at a lower scattering vector than that observed[23,24] for hydroxypropyl cellulose ($s \sim 0.55$ Å^{-1}) due to the greater length of the substituted side chains and indicates a level of correlation extending over some 50 Å^{-1}. The diffuse peak at $s \sim 1.5$ Å^{-1} relates to correlations within the chain segments, both within the cellulose backbone and the side chains. The scattering data of *Figure 3* show that there is a slight depression in the intensity of the peak at $s = 0.5$ Å^{-1} for samples with high crosslinking density. This is not so surprising and indicates that the crosslinking chains have disrupted to a certain extent the spatial correlation between neighbouring chain molecules.

The liquid crystal state is particularly sensitive to the application of external fields and liquid crystal elastomers are no exception[3,4,22]. We have utilized the anisotropy in the X-ray scattered intensity at ~ 0.5 Å^{-1} to obtain a measure of the degree of global orientation in the sample which develops as a result of the application of differing mechanical strain. The global orientation parameter takes account of both the lack of complete orientational order within a particular region and the variation in the director orientation throughout the sample. At zero strain the director pattern is isotropic and hence $\langle P_2 \rangle$ is zero. The degree of orientation achieved depends both upon the temperature of deformation and the extension ratio employed. The global orientation parameter $\langle P_2 \rangle$ is plotted as a function of the applied strain for elastomer D at a temperature of 50°C in *Figure 4*. The curve follows a similar trend reported for side-chain liquid crystal elastomers[3,4,22] in that there is a smooth development of orientation until a plateau is reached. The level of orientation in the plateau region should correspond to the order parameter of the liquid crystal phase, i.e. we should now have a monodomain. Two factors are of particular note in *Figure 4*. The first is the overall scale of orientation. This is much lower than might be expected. However, it is important to remember that the value of orientation in *Figure 4* relates to the anisotropy of the X-ray scattering. No corrections have been made for the intrinsic azimuthal width of a perfectly aligned system[21]. Estimating such corrections is far from being straightforward in a system with such a complex side-chain structure. The second point is that the rate of orientation development with strain is less marked than

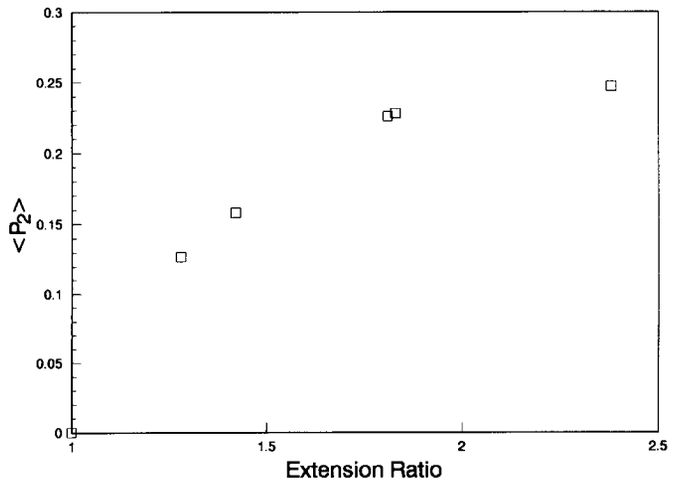

Figure 4 A plot of the orientation parameter $\langle P_2 \rangle$ against the extension ratio at a temperature of 50°C for elastomer sample D

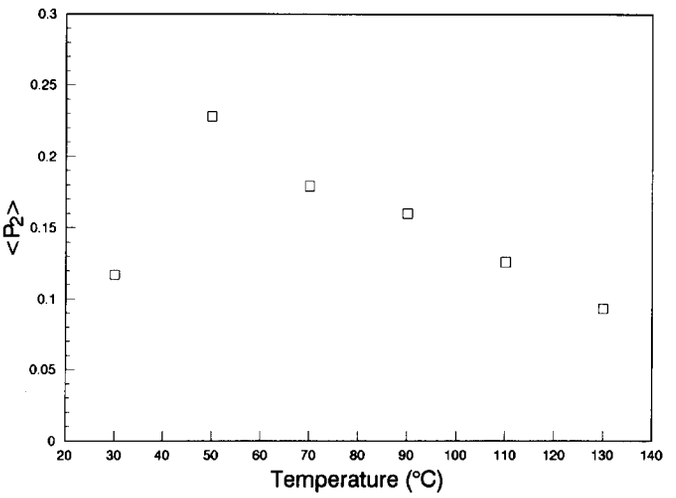

Figure 5 A plot of orientation parameter against the stretching temperature for an extension ratio of 1.75 for elastomer sample D

that observed for side-chain liquid crystal elastomers[3,22]. In other words here the extension ratio required to reach the plateau is ~ 1.7–2.0 whereas for a side-chain liquid crystal elastomer the equivalent extension ratio was 1.3–1.5. It might have been expected that since the coupling between the network and the liquid crystal structure is direct in a main-chain system, that stress–orientation effects would be more marked than for the indirectly coupled side-chain systems. Since the plateau level of orientation corresponds to the order parameter of the liquid crystal system, we should expect that this is sensitive to the temperature during extension. *Figure 5* shows the orientation achieved at constant strain for differing temperatures. The strain was chosen to reflect the plateau orientation effects. There is a significant increase in orientation achieved as the deformation temperature is lowered. However below 50°C kinetic effects dominate as a lower level of orientation is reached. This reduction may be related to the approaching glass transition.

A characteristic of elastomer systems is their ability to swell considerably in appropriate 'solvents', the extent of swelling being a balance between the decreasing entropy of the network and the solvent–network interactions. For liquid crystal systems there is an extra factor arising from the stability of the liquid crystal phase and for a rigid rod system the role of the chain in terms of configurational entropy is much reduced. The elastomers prepared here could be swollen in acetone or benzene. Thin sections cut from the incompletely swollen material exhibited weak birefringent textures when observed in the polarizing optical microscope. Thus in acetone or benzene, the crosslinked material exhibits a lyotropic phase as did a similar uncrosslinked propanoate ester of hydroxypropyl cellulose[15]. Upon removal of the solvent, the solid polymer was recovered which reproduced the thermotropic behaviour described above. For a particular system it was found that steady state levels of swelling were achieved at room temperature in a matter of minutes. Even at swelling level $> 500\%$ w/w the swollen material was not optically clear, and displayed birefringent textures indicative of a liquid crystal phase. Swollen samples behaved elastically and again high levels of stable birefringence could be obtained by application of stress fields and such additional

birefringence was eliminated by removal of the stress. *Figure 6* shows the X-ray scattering curve for such a swollen sample in a steady state sealed between mica windows, in comparison to the unswollen material. This shows no sharp peaks indicative of a microcrystalline structure. In all swollen systems the diffuse peak in the scattering pattern at $s \sim 0.5\,\text{Å}^{-1}$ was absent. For the solid samples this peak was related to the interchain correlations. Clearly, in the swollen materials the absence of the peak indicates that the solvent is uniformly distributed through the sample. In other words the chains are completely disassociated from each other, and hence the birefringence does not arise from small regions of highly correlated regions. The peak at $s \sim 1.5\,\text{Å}^{-1}$ is broader than for the solid film since now the principal contribution arises from the liquid acetone. The total extent of swelling of the elastomers in benzene at 20°C ranged from a ratio of 9.9 for sample B to 6.6 for sample E.

A series of experiments were performed to assess the effect of crosslinking on the stability of the liquid crystal phase in the swollen state. It was found that the birefringent textures observed in the optical microscope disappeared when the swelling ratio exceeded ~5 or a concentration of the polymer in the solvent of some 20% v/w. The effect of the crosslinking density on the critical swelling level at which the birefringent texture disappears is shown in *Figure 7*. The increasing swelling level with increasing crosslinking density indicates that more swellant is needed to destabilize the lyotropic liquid crystal phase for those samples having a higher crosslinking density. The observed birefringent texture indicates the existence of a liquid crystal phase. The concentration of the cellulose derivative in these swollen lyotropic liquid crystal elastomers is somewhat lower than that required to produce a liquid crystal phase in an uncrosslinked system[15,25]. The extended nature of the cellulose chains, the prerequisite to the formation of the liquid crystal phases, means that there is little

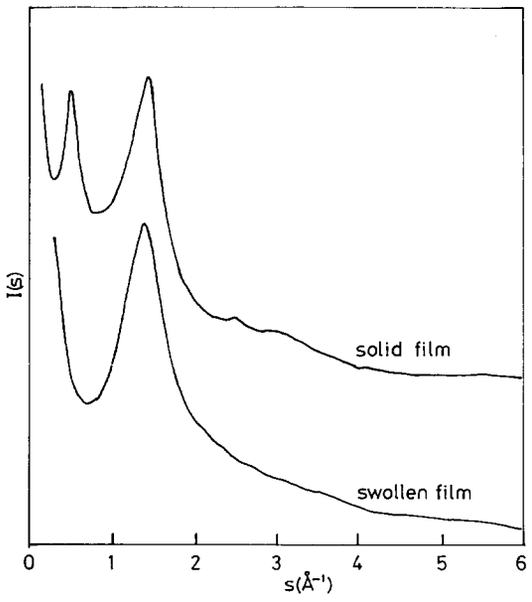

Figure 6 X-ray scattering curves for a cellulose-based elastomer without solvent at room temperature and the same elastomer swollen in acetone. The latter curve was obtained at room temperature for a sample sealed in a cell with mica windows to prevent loss of acetone. The curves have been arbitrarily offset along the vertical axis

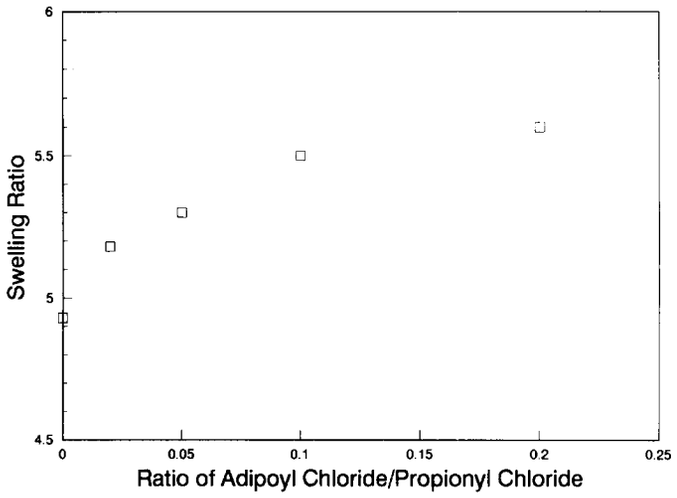

Figure 7 A plot of critical swelling ratio of the crosslinked cellulose materials and benzene swellant against the nominal crosslinking density. Above this swelling ratio the swollen samples are isotropic

configurational entropy lost on swelling in contrast to conventional crosslinked networks. The limit of swelling must be largely determined by the stability of the liquid crystal phase. The low concentration of the polymer in the swollen material suggests an enhancement of the chain stiffness as the source of greater stability of the lyotropic phase compared with uncrosslinked materials. However it is difficult to reconcile the observations of *Figure 7* unless the material was present in some liquid crystal like ordering state at the crosslinking stage. A similar observation may be made of the data presented in *Table 2*. The introduction of crosslinking into the liquid crystal phase will only stabilize and enhance that phase if the crosslinking was performed in the liquid crystal or a more ordered phase[6,26]. A system crosslinked in solution or in an isotropic melt would require a deformation of the network in order to achieve a high level of orientational ordering, and such deformation would be expected to lead to a depression of the nematic–isotropic transition temperature or critical swelling ratio. The conditions of esterification were such that if the cellulose-based polymer was uniformly dispersed through the reaction vessel, the concentration would be well below that required for the formation of a liquid crystal phase. Observations of the material in the reaction vessel suggest that parts of the material especially after crosslinking when the solubility would be much reduced could have concentrations above the critical level, although of course crosslinking reactions may be less likely in such regions. However it is difficult to extend such possibilities to the complete sample. The most reasonable explanation relates to the vigorous stirring employed during the derivatization reactions. Even though the solution employed was relatively dilute, it was particularly viscous. The stirring could lead to chain extension and some alignment. The crosslinking of such a solution could lead to the observations described above.

SUMMARY

The introduction of controlled levels of crosslinking into derivatives of cellulose leads to materials with interesting properties. With suitable fractions of crosslinking these

cellulose-based elastomers exhibit both reversible lyotropic and thermotropic liquid crystal behaviour. The introduction of crosslinking appears to stabilize the liquid crystal phase and we relate this to the condition of the cellulose derivative system in the reaction vessel. Although the crosslinking raises the liquid crystal to isotropic transition temperature and the critical ratio of swelling it also appears to inhibit the clear formation of a cholesteric phase. These cellulose-based liquid crystal elastomers exhibit the phenomena of mechanically induced molecular switching, although it is less marked than in other liquid crystal systems. Cellulose derivatives suffer from the problems of broad molecular weight ranges and the introduction of crosslinking can only complicate an already inhomogeneous system. These factors reveal themselves in the broad transitions and rather blurred behaviour. Although recently there have been some predictions for the behaviour of a network composed of rigid rods[27], an understanding of the influence of the various factors upon the mechanical properties and in particular the development of global orientation is some way off. At present we are pursuing alternative routes to network formation which may clarify both the phase transition and phase stability data and the mechanical properties.

ACKNOWLEDGEMENTS

This work is supported by the Science and Engineering Research Council (GR/F08405). We are grateful to Hercules for the gift of the hydroxypropyl cellulose.

REFERENCES

1 Zentel, R. *Liq. Cryst.* 1986, **1**, 589
2 Barnes, N. R., Davis, F. J. and Mitchell, G. R. *Mol. Cryst. Liq. Cryst.* 1989, **168**, 13
3 Davis, F. J. and Mitchell, G. R. *Polym. Commun.* 1987, **28**, 8
4 Mitchell, G. R., Davis, F. J. and Ashman, A. S. *Polymer* 1987, **28**, 639
5 Kock, H. J., Finklemann, H., Gleim, W. and Rehage, G. in 'Polymer Science and Technology' (Ed. A. Blumstein), Vol. 28, Plenum, New York, 1983
6 Warner, M., Gelling, K. P. and Vilgis, T. A. *J. Chem. Phys.* 1988, **88**, 4008
7 Davis, F. J. and Mitchell, G. R. *Polymer* submitted
8 Zentel, R. and Reckert, G. *Makromol. Chem.* 1986, **187**, 1915
9 Davis, F. J., Gilbert, A., Mann, J. and Mitchell, G. R. *J. Polym. Sci., Polym. Chem. Edn* 1990, **28**, 1455
10 Hanus, K. H. and Pechhold, W. *Colloid Polym. Sci.* 1990, **268**, 222
11 Barnes, N. R. and Mitchell, G. R. *Liq. Cryst.* submitted
12 Werbowyj, R. S. and Gray, D. G. *Mol. Cryst. Liq. Cryst. (Lett.)* 1976, **34**, 97
13 Gray, D. G. *J. Appl. Polym. Sci. Symp.* 1983, **37**, 179
14 Sixou, P. and Ten Bosch, A. in 'Cellulose, Structure, Modification and Hydrolysis' (Eds R. A. Young and R. M. Rowell), Wiley, New York, 1986
15 Tseng, S-L., Laivins, G. V. and Gray, D. G. *Macromolecules* 1982, **15**, 1262
16 Bhadani, S. N. and Gray, D. G. *Makromol. Chem. Rapid Commun.* 1982, **3**, 449
17 Bhadani, S. N. and Gray, D. G. *Mol. Cryst. Liq. Cryst. (Lett.)* 1984, **102**, 225
18 Suto, S. *J. Appl. Polym. Sci.* 1989, **37**, 2781
19 Klug, E. D. in 'Encyclopedia of Polymer Science and Technology' (Ed. N. M. Bikales), Vol. 15, Interscience, New York, 1971, p. 307
20 Lovell, R. and Mitchell, G. R. *Acta Cryst.* 1981, **A37**, 135
21 Mitchell, G. R. in 'Comprehensive Polymer Science' (Eds G. Allen, J. G. Bevington, C. Booth and C. Price), Vol. 1, Pergamon Press, 1989, Ch. 31
22 Guo, W., Davis, F. J. and Mitchell, G. R. in preparation
23 Samuels, R. J. *J. Polym. Sci.* 1969, **A2**, 1197
24 Shimamura, K., White, J. L. and Fellers, J. F. *J. Appl. Polym. Sci.* 1981, **26**, 2166
25 Tseng, S-L., Valente, A. and Gray, D. G. *Macromolecules* 1981, **14**, 715
26 de Gennes, P. G. *C.R. Acad. Sci. Ser.* 1975, **B281**, 101
27 Jones, J. L. and Marques, C. M. *J. Phys. (France)* 1990, **51**, 1113